ARCHIVES OF ACOUSTICS
23, 4, 521–531 (1998)

# PIEZOELECTRIC INTERFACIAL WAVES IN TWO-MEDIUM STRUCTURES

W. LAPRUS

Polish Academy of Sciences,
Institute of Fundamental Technological Research
(00-049 Warszawa, Świętokrzyska 21, Poland)

The theory is given and a numerical analysis is presented of propagation of piezoelectric interfacial waves along a perfectly conducting plane that separates two piezoelectric half-spaces of different crystallographic orientations or two half-spaces of different piezoelectrics. In the case of slightly different orientations (half a degree in each Euler angle), it is found that the coupling coefficient is in general less than in the case of two half-spaces of the same orientation, but still large. For example, it is 3.40% for lithium niobate (instead of 3.50%), 0.85% for dilithium tetraborate (instead of 0.90%), 0.15% for langasite (instead of 0.20%). In the case of two half-spaces of arbitrary different crystallographic orientations (lithium niobate and lithium niobate), and two half-spaces of different piezoelectrics (dilithium tetraborate and lithium niobate), it is found that the coupling coefficient may be quite large for some crystal cuts (correspondingly 2.25% and 1.45%), although for the majority of crystal cuts the waves do not exist.

## 1. Introduction

The piezoelectric interfacial wave (PIW) is guided by a perfectly conducting plane embedded in a piezoelectric medium [3, 4]. The guiding structure can be produced by cutting a piezoelectric crystal into two pieces, covering the faces of the cut with metal, and bonding the two pieces together. In this process, some misalignment of the crystallographic axes of the two pieces is inevitable (up to about half a degree in each Euler angle). In view of applications, it is important to know if such an error does not affect adversely the existence and properties of PIW.

In the paper, a numerical analysis of misalignment is presented for several piezoelectrics. The electro-mechanical field equations are transformed to a system of first-order ordinary differential equations [5, 11]. The associated eigenvalue problem is solved numerically for many orientations of the conducting plane with respect to the crystallographic axes and for different types of misalignment. It is found that piezoelectric interfacial waves with a high coupling coefficient are relatively insensitive to misalignment. In general, however, the domains of existence in the space of Euler angles are smaller than in the case without misalignment.

Next, two-medium guiding structures of two kinds are investigated. The first consists of a perfectly conducting interface and two piezoelectric half-spaces of arbitrary different

crystallographic orientations (this is a generalization of the basic structure with misalignment). The second consists of a perfectly conducting interface and two half-spaces of different piezoelectrics. Calculations are performed for variable crystallographic orientation of one half-space (lithium niobate or dilithium tetraborate) and a fixed orientation of the other (lithium niobate). The domains of existence of PIW are determined, and wave propagation parameters are calculated for selected orientations. It is found that small isolated domains may exist in the angle space, where PIW piezoelectric coupling is high.

## 2. Theoretical background

We assume that the electro-mechanical field depends on time through the factor $\exp(j\omega t)$. In the system of coordinates $(x, y, z)$ the field satisfies the equations given in Ref. [11]. We shall adopt the notations and conventions of Ref. [11].

The medium is described by the following constants: elastic tensor $c_{ijkl}$, piezoelectric tensor $e_{kij}$, dielectric tensor $\varepsilon_{ki}$, and mass density $\varrho$. The field variables are: particle displacement $u_i$, electric potential $\phi$, stress tensor $T_{ij}$, and electric displacement $D_k$.

Let us consider two homogeneous piezoelectric half-spaces (for $z > 0$ and $z < 0$), and the perfectly conducting plane $z = 0$, as shown in Figure 1. We assume that the field is independent of $y$, and that the dependence on $x$ and $z$ is given by the factor $\exp(-j\omega r x - j\omega s z)$.

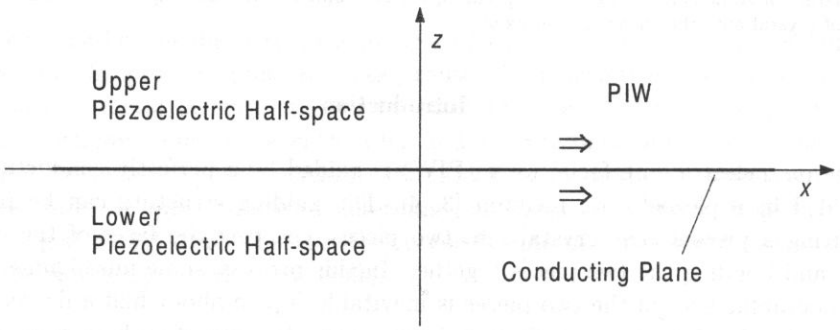


Fig. 1. The system of coordinates.

In each half-space the field equations can be reduced to a system of eight linear algebraic equations [11]. The following eight field variables will be used: particle displacement $u_i$, electric potential $\phi$, traction force $T_i = T_{3i}$ at the interface, and normal (to the interface) component $D_3$ of the electric displacement $D_i$. We have

$$H_{KL}(r)F_L = qF_K\,, \tag{1}$$

where $K, L = 1, \ldots, 8$, $(F_K) = (j\omega r u_i, j\omega r\phi, T_i, D_3)$, and $q = s/r$. To each half-space corresponds a matrix $H_{KL}$ which is real and nonsymmetric ($r$ is assumed to be real). It depends on material constants [11].

After solving the eigenvalue problem defined by Eq. (1) we get eight eigenvectors $\tilde{F}_K^{(J)}(r)$ corresponding to eight eigenvalues $q^{(J)}(r)$ for $J = 1, \ldots, 8$. The $J$th eigenwave has the form

$$F_K^{(J)} = \tilde{F}_K^{(J)} \exp(j\omega t - j\omega r(x + q^{(J)} z)). \tag{2}$$

The solution of the field equations in each half-space is a linear combination of the eigenwaves corresponding to that half-space.

The eigenvector $\tilde{F}_K^{(J)}$ will be called upper (lower) if either $\operatorname{Im} q^{(J)} < 0$ ($\operatorname{Im} q^{(J)} > 0$) or $\operatorname{Im} q^{(J)} = 0$ and the $z$ component of the real part of the Poynting vector is positive (negative). Note that $\operatorname{Im} q^{(J)} \neq 0$ for $J = 1, \ldots, 8$ if $r > r_c$ where $r_c$ is the cutoff slowness of bulk waves. In each half-space the set of eigenvectors consists of four upper and four lower eigenvectors.

The surface wave field vanishes at infinity, and there is no energy flux to the boundary (no sources in the space). Therefore, the solution $F_K^+$ of the field equations in the upper half-space consists of upper eigenwaves for that half-space, and the solution $F_K^-$ in the lower half-space consists of lower eigenwaves for that half-space. At the plane $z = 0$, the complex amplitudes of the two solutions are

$$\tilde{F}_K^{\pm} = \pm \sum_J^{\pm} C_J \tilde{F}_K^{(J)} \tag{3}$$

where the set of the eight eigenvectors $\tilde{F}_K^{(J)}$ for $J = 1, \ldots, 8$ consists of four upper eigenvectors for the upper medium and four lower eigenvectors for the lower medium. The plus (minus) superscript of the sum symbol means that the summation is performed over $J$ such that $\tilde{F}_K^{(J)}$ is an upper (lower) eigenvector for the upper (lower) half-space. The minus sign before the sum symbol in Eq. (3) is used to simplify some formulas considered later. The coefficients $C_J$ are to be determined from boundary conditions.

The field equations can be solved in each half-space separately, provided appropriate boundary conditions are imposed at the plane $z = 0$. In general, the boundary conditions may determine either the jumps of amplitudes $\Delta\tilde{F}_K = \tilde{F}_K^+ - \tilde{F}_K^-$, or the amplitudes $\tilde{F}_K^+$ (or $\tilde{F}_K^-$). Below, it will be shown that the two sets of values are related to each other.

Let $R_{KJ} = \tilde{F}_K^{(J)}$, and denote by $L_{JK}$ the inverse of the matrix $R_{KJ}$. From Eq. (3) it follows that

$$\Delta\tilde{F}_K = R_{KJ} C_J \,, \tag{4}$$

and hence

$$C_J = L_{JK}\, \Delta\tilde{F}_K \,. \tag{5}$$

Using Eq. (5) we write Eq. (3) as

$$\tilde{F}_K^{\pm} = Z_{KL}^{\pm}(r)\, \Delta\tilde{F}_L \,, \tag{6}$$

where

$$Z_{KL}^{\pm}(r) = \pm \sum_J^{\pm} R_{KJ} L_{JL} \,. \tag{7}$$

The plus or minus superscript of the sum symbol has the same meaning as in Eq. (3) (columns of the matrix $R_{KJ}$ are eigenvectors of the two matrices $H_{KL}$). $R_{KJ}$ and $L_{JL}$,

and thereby $Z^{\pm}_{KL}$, depend on $r$. The matrices $Z^{+}_{KL}$ and $Z^{-}_{KL}$ are related to each other. Indeed, we have

$$\Delta\tilde{F}_K = \tilde{F}^{+}_K - \tilde{F}^{-}_K = (Z^{+}_{KL} - Z^{-}_{KL})\,\Delta\tilde{F}_L\,, \tag{8}$$

which means that

$$Z^{+}_{KL} - Z^{-}_{KL} = I_{KL}\,, \tag{9}$$

where $I_{KL}$ is the identity matrix. Thus, off-diagonal elements of the two matrices are equal.

Equation (6) is a fundamental relation in the problem of PIW propagation. It should be satisfied by the field variables at the boundary of each piezoelectric half-space, irrespective of what boundary conditions are imposed there. The matrices $Z^{+}_{KL}(r)$ and $Z^{-}_{KL}(r)$ are determined completely by the set of eigenvectors for a given $r$. Therefore, they are characteristic of the both media rather than of any particular solution of the field equations.

We assume that all the field variables are continuous across the plane $z = 0$ except $D_3$. The amplitude $\tilde{D}_3$ suffers a jump $\Delta\tilde{D}_3$ (assumed to be real). For $K = 4$, Eq. (6) gives

$$j\omega r\tilde{\phi} = Z(r)\,\Delta\tilde{D}_3\,, \tag{10}$$

where $\tilde{\phi} = \tilde{\phi}^{+} = \tilde{\phi}^{-}$ is the amplitude of the electric potential at the interface, and $Z(r) = Z^{+}_{48}(r) = Z^{-}_{48}(r)$ is a complex-valued function. 1/Z has the physical dimension of the dielectric permittivity. This is more clearly seen if we rewrite Eq. (10) in the form

$$\tilde{E}_1 = Z(r)\,\Delta\tilde{D}_3\,. \tag{11}$$

$E_1 = -\partial\phi/\partial x$ is the tangential (to the interface) component of the electric field. This component should vanish at the perfectly conducting interface which implies that $\phi = 0$ for $z = 0$.

The function $Y(r) = 1/Z(r)$ is a counterpart of the effective permittivity function in the theory of surface acoustic waves [1, 2].

It can be shown that $\operatorname{Re} Z(r)$ is equal to zero for $r > r_c$, and that $\operatorname{Im} Z(r)$ tends to a positive number as $r \to \infty$. Here and below, by $r_c$ we mean the greater of the two values of $r_c$ corresponding to the two half-spaces. PIW exists if the dispersive equation $Z(r) = 0$ is satisfied for a particular value of $r$, say $r_p$. Then $\tilde{\phi} = 0$, i.e. $\phi$ satisfies the boundary condition for $z = 0$, and $r_p$ is the slowness of PIW.

## 3. Numerical analysis

In each half-space the orientation of crystallographic axes is determined by a triplet of Euler angles. Triplets of angles may be represented as points in a three-dimensional space. The solution of the dispersive equation $Z(r) = 0$ depends on the crystallographic orientation of the both piezoelectric half-spaces, i.e. it depends on two triplets of Euler angles.

The effect of misalignment is calculated as follows. First, assuming that there is no misalignment, we scan the three-dimensional space of Euler angles at discrete points

so that the angles change in steps of 4°. Then, for each scanned point, we rotate the upper and/or lower half-space in a sequence of six separate rotations which correspond to differences of 0.5° in Euler angles between the two half-spaces: differences in one Euler angle (three rotations), and differences in two Euler angles (three rotations). These rotated configurations are intended to simulate random misalignment.

The symmetry of piezoelectric crystals implies that it is sufficient to scan the following ranges: 0°–30°, 0°–180°, 0°–180° for trigonal crystals (and orthorhombic Rochelle salt), and 0°–45°, 0°–180°, 0°–180° for cubic crystals.

For each chosen set of six Euler angles, the two eigenvalue problems are solved numerically (using EISPACK routines [6]) for several values of $r$ in search of the two $r_c$ (simple zero-finding routine). Next, the eigenvalue problems are solved for several values of $r$ in a small neighborhood of the greater of the two $r_c$, just above it, in search of $r_p$ (zero-finding routine applied to the function $Z(r)$). If $Z(r)$ has no zero for a rotated configuration, then calculations are stopped and it is considered that PIW does not exist at that particular scanned point.

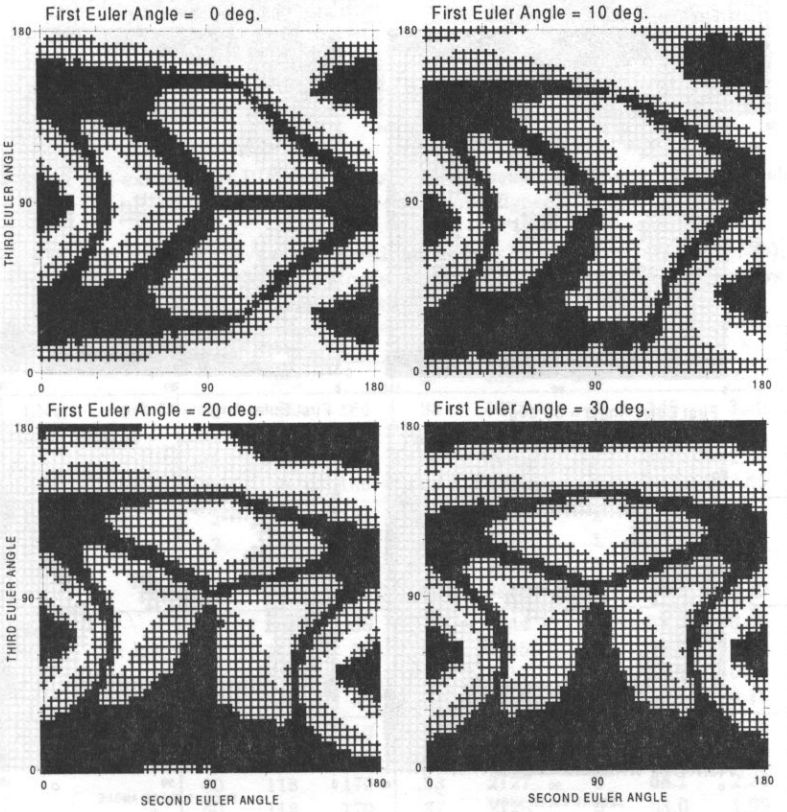


Fig. 2. Domains of non-existence of PIW for lithium niobate (*black squares*: half-spaces aligned, *black squares* and *crosses*: half-spaces misaligned).

If PIW exists then its parameters are calculated: $\delta = (r_p - r_c)/r_c$, phase velocity $v_p = 1/r_p$, beam steering angle $\psi$, effective permittivity $\varepsilon_{eff}$, piezoelectric coupling coefficient $\kappa$ (definitions of the last three parameters are given in Ref. [11]). The calculations are performed for $\omega = 10^6\,s^{-1}$. The material constants for the piezoelectrics are taken from Refs. [7] and [8].

The effect of misalignment for lithium niobate, dilithium tetraborate, langasite, and Rochelle salt is illustrated in Figures 2 to 5. Some asymmetry of the patterns (especially well seen for the first Euler angle equal to 0° and to 30° or 45°) is an effect of finite precision of calculation. Domains of non-existence of PIW without misalignment are shown more precisely (due to scanning in steps of 2°) in figures which can be found in Refs. [9]-[11]. The figures are detailed symbolic maps of PIW properties (without misalignment) for lithium niobate, dilithium tetraborate, langasite, and other piezoelectrics. Color versions of these maps are published on the Internet [12].

Table 1 compares PIW parameters without misalignment to those with misalignment. For each medium, parameters at two points of the angle space are given (representative

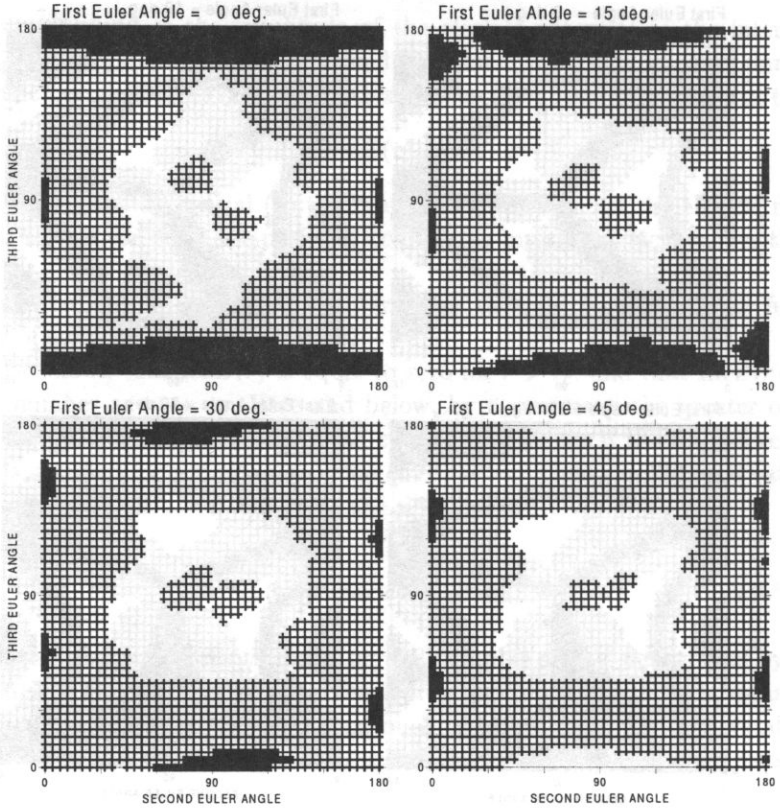


Fig. 3. Domains of non-existence of PIW for dilithium tetraborate (*black squares*: half-spaces aligned, *black squares* and *crosses*: half-spaces misaligned).

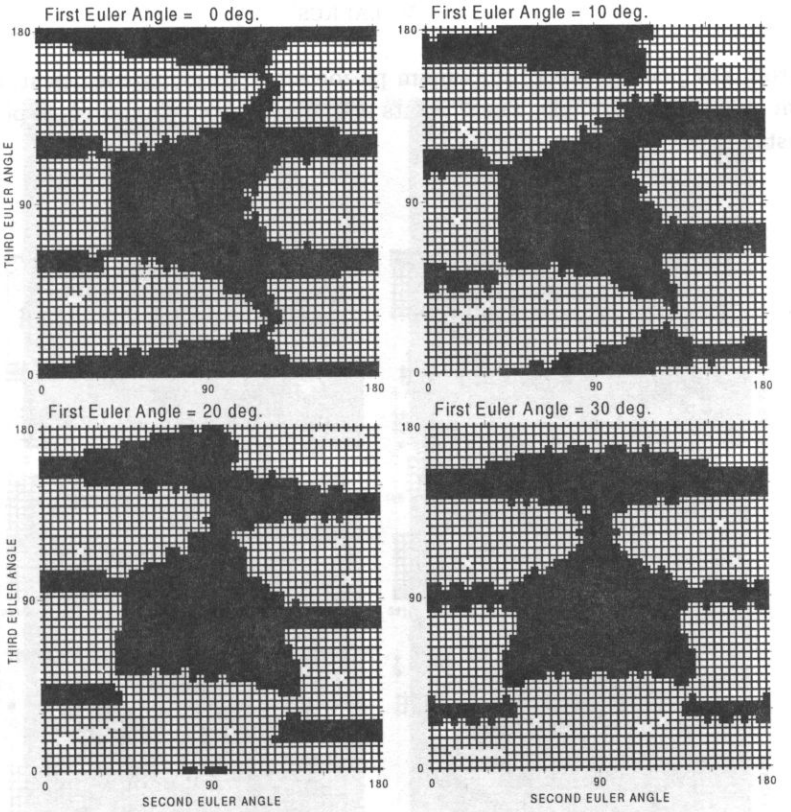


Fig. 4. Domains of non-existence of PIW for langasite (*black squares*: half-spaces aligned, *black squares* and *crosses*: half-spaces misaligned).

**Table 1.** Effect of misalignment (rows marked with an asterisk) for lithium niobate (LNO), dilithium tetraborate (LBO), langasite (LGS), and Rochelle salt (LRS). For reference, parameters of PIW without misalignement are also given (rows without asterisk).

| medium | Euler angles | | | $\delta$ | $v_p$ | $\psi$ | $\varepsilon_{eff}$ | $\kappa$ |
|---|---|---|---|---|---|---|---|---|
| | deg | | | % | m/s | deg | – | % |
| LNO | 30 | 88 | 164 | .38 | 4075 | −3 | 149. | 3.50 |
| * | 30 | 88 | 164 | .39 | 4074 | −3 | 149. | 3.40 |
| | 28 | 96 | 166 | .04 | 4081 | 0 | 150. | 2.30 |
| * | 28 | 96 | 166 | .05 | 4081 | 0 | 149. | 2.65 |
| LBO | 2 | 88 | 124 | .48 | 3299 | 2 | 18.7 | 0.90 |
| * | 2 | 88 | 124 | .33 | 3298 | 1 | 18.7 | 0.85 |
| | 10 | 90 | 90 | .39 | 3873 | 0 | 18.8 | 0.75 |
| * | 10 | 90 | 90 | .06 | 3868 | 4 | 18.8 | 0.50 |
| LGS | 8 | 144 | 36 | .13 | 2944 | −1 | 58.0 | 0.20 |
| * | 8 | 144 | 36 | .01 | 2945 | −9 | 58.0 | 0.10 |
| | 10 | 148 | 38 | .11 | 2917 | 0 | 59.1 | 0.20 |
| * | 10 | 148 | 38 | .03 | 2919 | −4 | 59.1 | 0.15 |
| LRS | 60 | 66 | 12 | .47 | 2120 | 0 | 70.0 | 2.00 |
| * | 60 | 66 | 12 | .50 | 2120 | 1 | 70.1 | 2.40 |
| | 60 | 118 | 170 | .53 | 2127 | 0 | 68.1 | 2.20 |
| * | 60 | 118 | 170 | .37 | 2126 | 0 | 68.0 | 1.95 |

of two groups of points): one of maximum piezoelectric coupling coefficient, and one of minimum beam steering angle. These points are selected from thousands of points where PIW exists.

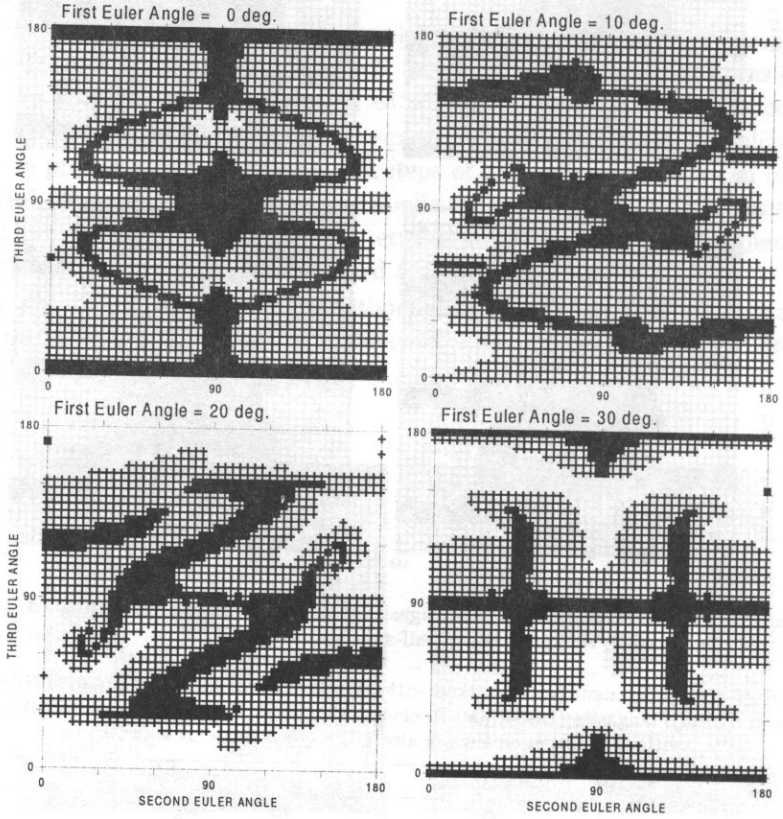


Fig. 5. Domains of non-existence of PIW for Rochelle salt (*black squares*: half-spaces aligned, *black squares* and *crosses*: half-spaces misaligned).

For two half-spaces of arbitrary different crystallographic orientations and two half-spaces of different piezoelectrics, PIW propagation parameters are calculated using the procedures that are described above. In the both cases, the lower piezoelectric is lithium niobate of a fixed orientation (Euler angles: 30°, 88°, 164°), and the upper piezoelectric has a variable orientation (the scanning of the angle space in steps of 4° is performed). The fixed orientation gives high piezoelectric coupling of PIW in lithium niobate without misalignment, i.e. when the both half-spaces have that orientation.

The maps of PIW properties for each case are shown in Figures 6 and 7. PIW parameters are given in Table 2 for each case at two points of the angle space: one of maximum piezoelectric coupling coefficient, and one of minimum beam steering angle.

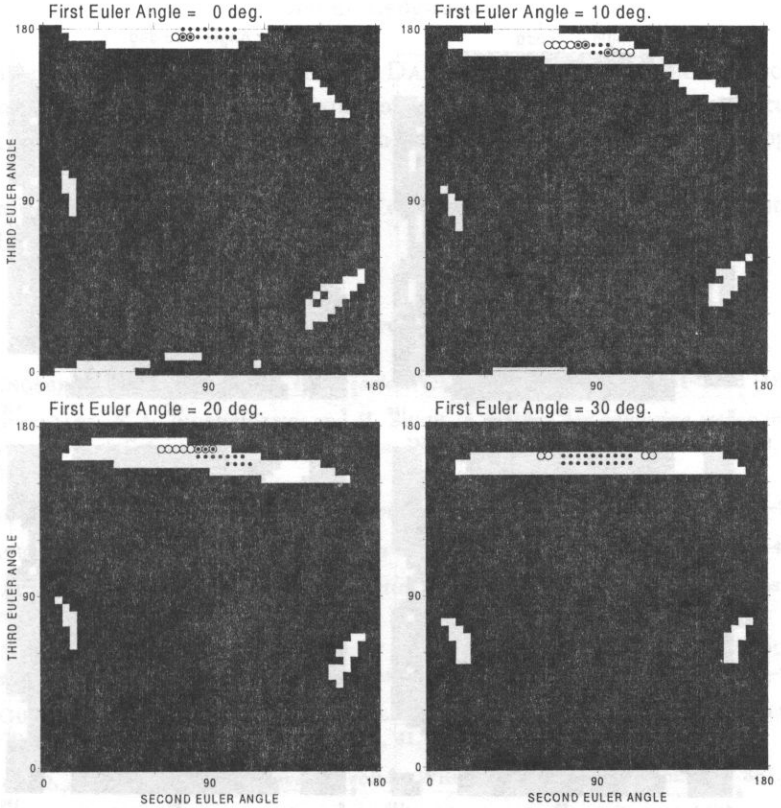


Fig. 6. Maps of PIW properties for lithium niobate of fixed orientation in the lower half-space (Euler angles: 30°, 88°, 164°) and lithium niobate of variable orientation in the upper half-space (*black squares*: no PIW, *dots*: PIW coupling coefficient > 2%, *circles*: PIW coupling coefficient > 1% and PIW beam steering angle < 0.5°).

**Table 2**. PIW parameters for two piezoelectric half-spaces of different orientations (lithium niobate and lithium niobate) and of different media (dilithium tetraborate and lithium niobate). In the both cases lithium niobate in the lower half-space has the same orientation (Euler angles 30°, 88°, 164°) and the orientation of the upper half-space is given in the table.

| medium | Euler angles | | | $\delta$ | $v_p$ | $\psi$ | $\varepsilon_{eff}$ | $\kappa$ |
|---|---|---|---|---|---|---|---|---|
| | deg | | | % | m/s | deg | – | % |
| LNO/LNO | 30 | 88 | 164 | 0.38 | 4075 | −3 | 149. | 3.45 |
| | 20 | 88 | 168 | 0.12 | 4074 | 0 | 151. | 2.25 |
| LBO/LNO | 0 | 84 | 152 | 1.05 | 4048 | −31 | 76.6 | 2.60 |
| | 15 | 20 | 152 | 0.56 | 4067 | 0 | 74.9 | 1.45 |

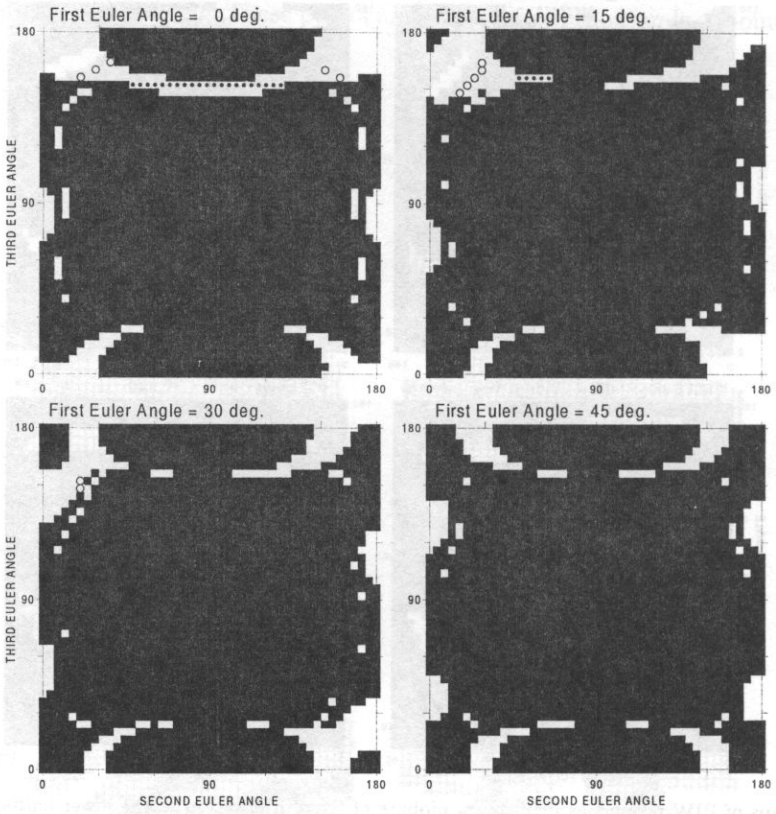


Fig. 7. Maps of PIW properties for lithium niobate of fixed orientation in the lower half-space (Euler angles: 30°, 88°, 164°) and dilithium tetraborate of variable orientation in the upper half-space (*black squares*: no PIW, *dots*: PIW coupling coefficient > 2%, *circles*: PIW coupling coefficient > 1% and PIW beam steering angle < 0.5°).

## 4. Conclusion

From Figures 2 to 5 it is seen that misalignment affects mainly PIW propagation for those points in the angle space (i.e. those crystal cuts) for which piezoelectric coupling is low. Domains of existence of PIW are smaller, sometimes much smaller, than in the case without misalignement. Nevertheless, as Table 1 proves, the piezoelectric coupling coefficient remains large if it is large without misalignment. Therefore, in applications, when crystall cuts of high coupling are selected, misalignment is not very important.

In contrast to one-medium structures, two-medium structures are characteristic of extremely small domains of existence of PIW. In fact, for other pairs of piezoelectrics, which have also been analyzed, PIW seems not to exist at all (perhaps a scanning in smaller steps would reveal PIW existence). But still there are small domains of high piezoelectric coupling, as seen in Figures 6 and 7. The piezoelectric coupling coefficients shown in Table 2 are comparable with those for one-medium structures.

## Acknowledgment

The author would like to thank Prof. E. DANICKI for suggesting the research of PIW propagation in the presence of misalignment, and for discussing technical problems of producing crystal cuts of a given orientation, which is important in view of applications of PIW.

This work was supported by Committee of Scientific Research (Poland) under Grant No. 2P03B 171 12.

## References

[1] K.A. INGEBRIGTSEN, *Surface waves in piezoelectrics*, J. Appl. Phys., **40**, 2681–2686 (1969).

[2] K. BLØTEKJAER, K.A. INGEBRIGTSEN and H. SKEIE, *A method for analyzing waves in structures consisting of metal strips on dispersive media*, IEEE Trans. Electron Devices, **ED-20**, 1133–1138 (1973).

[3] E. DANICKI, *New interfacial shear waves in piezoelectrics*, Appl. Phys. Lett., **64**, 969–970 (1994).

[4] E. DANICKI, *Piezoelectric interfacial waves in* $LiNbO_3$", Appl. Phys. Lett., **66**, 3439–40 (1995).

[5] E.L. ADLER, *SAW and pseudo-SAW properties using matrix methods*, IEEE Trans. Ultrason. Ferroel. Freq. Control, **41**, 699–705 (1994).

[6] B.T. SMITH, J.M. BOYLE, B. S. GARBOW, Y. IKEBE, V. C. KLEMA, AND C. B. MOLER, *Matrix eigensystem routines – EISPACK Guide*, Lecture Notes in Computer Science, **6**, 149–258 (1974).

[7] J.G. GUALTIERI, J.K. KOSINSKI and A. BALLATO, *Piezoelectric materials for SAW applications*, IEEE Trans. Ultrason. Ferroel. Freq. Control, **41**, 53–59 (1994).

[8] B.A. AULD, *Acoustic fields and waves in solids*, Wiley, New York 1973, Vol. 1, p. 357.

[9] E. DANICKI and W. LAPRUS, *Piezoelectric interfacial waves in langasite and dilithium tetraborate*, [in:] 1995 IEEE Ultrasonics Symposium Proceedings, M. LEVY, S.C. SCHNEIDER and B.R. MCAVOY [Eds.], IEEE, New York 1995, pp. 1011–1014.

[10] E. DANICKI and W. LAPRUS, *Piezoelectric interfacial waves in langasite and dilithium tetraborate*, Archives of Acoustics, **21**, 99–107 (1996).

[11] W. LAPRUS and E. DANICKI, *Piezoelectric interfacial waves in lithium niobate and other crystals*, J. Appl. Phys., **81**, 855–861 (1997).

[12] www.ippt.gov.pl/~wlaprus.